

Electronic Supplementary Information (ESI)

Designing Cu-CoO heterostructure nanosheets for efficient electrooxidation of 5-hydroxymethylfurfural to 2,5-furandicarboxylic acid

Dongfang Ji,^a Wenke Wang,^a Ting Sang,^a Jingcheng Hao,^a Xiaoyu Zhang,^{*b} and
Zhonghao Li^{*a}

^a Key Laboratory of Colloid and Interface Chemistry, Ministry of Education, Shandong University, Jinan, 250100, China, E-mail: zhonghaoli@sdu.edu.cn

^b Zhejiang Carbon Neutral Innovation Institute & Moganshan Institute of ZJUT at Deqing, Zhejiang University of Technology, Hangzhou 310014, China, E-mail: zhangxiaoyu@zjut.edu.cn

Experimental Section

Materials and chemicals

Choline chloride (ChCl), oxalic acid ($\text{H}_2\text{C}_2\text{O}_4$), potassium chloride (KCl) and copper acetylacetone ($\text{C}_{10}\text{H}_{14}\text{CuO}_4$) were all obtained from Aladdin Chemistry Co., Ltd. Potassium hydroxide (KOH), Cobalt chloride hexahydrate ($\text{CoCl}_2 \cdot 6\text{H}_2\text{O}$) were purchased from Sinopharm Chemical Regent Co., Ltd. 5-hydroxymethylfurfural (HMF), 2,5-furandicarboxylic acid (FDCA), 5-formyl furan2-carboxylic acid (FFCA) and 5-hydroxymethyl-2-furan-carboxylic acid (HMFCA) were purchased from Alfa-Aesar. 2,5-diformyl furan (DFF) was purchased from Tokyo Chemical Industry Co., Ltd. 5 wt% nafion solution was purchased from the Sigma Co., Ltd. Carbon cloth was obtained from Changsha Lyrun Material Co., Ltd. Nafion 115 membrane was purchased from Wuhan GaossUnion technology Co., Ltd.

Synthesis of choline chloride/oxalic acid (ChCl/OA) DES

The deep eutectic solvent (DES) was synthesized according to the procedures specified in the existing literature.¹ To obtain the DES, equimolar amount of choline chloride (ChCl) and oxalic acid (OA) was mixed and magnetically stirred at 80 °C for 30 minutes.

Synthesis of Cu-CoO heterostructure nanosheets

The Cu-CoO products with varying initial Cu and Co ratios are labeled as Cu-CoO (x:y), where x:y represents the Cu/Co atomic ratio of the initial feed. To synthesize the Cu-CoO (1:3) product, the Cu/Co-based precursor was first prepared using a microwave-assisted DES approach. In a typical procedure, 21.5 mg $\text{C}_{10}\text{H}_{14}\text{CuO}_4$ and

58.5 mg $\text{CoCl}_2 \cdot 6\text{H}_2\text{O}$ were dissolved in 1mL ChCl/OA DES. This mixture was then subjected to ultrasonication at 60 °C until a well-dispersed pink solution was obtained. The precursor was generated by heating the above mixture under microwave for 10 s at 100 W. For comparison, we also synthesize the precursors by microwave heating for 15 and 20 s. The precursors were then gathered, repeatedly washed with ethanol, and dried in the vacuum at room temperature for 6 hours.

Subsequently, the dried precursors were placed in a quartz tube inside a tube furnace and heat-treated at 400 °C for 2 hours with a ramp rate of 10 °C min^{-1} in a nitrogen atmosphere to yield Cu-CoO nanosheets. Finally, the product was rinsed with water and ethanol before being dried in the vacuum drying oven.

For comparison, Cu-CoO (1:2) and Cu-CoO (1:4) products were also fabricated according to the above procedures. To synthesize Cu-CoO (1:2), 28.4 mg of $\text{C}_{10}\text{H}_{14}\text{CuO}_4$ and 51.6 mg of $\text{CoCl}_2 \cdot 6\text{H}_2\text{O}$ were employed, whereas for Cu-CoO (1:4), 17.3 mg of $\text{C}_{10}\text{H}_{14}\text{CuO}_4$ and 62.7 mg of $\text{CoCl}_2 \cdot 6\text{H}_2\text{O}$ were used. Moreover, CoO product was also synthesized with $\text{CoCl}_2 \cdot 6\text{H}_2\text{O}$.

Characterizations

The X-ray diffraction (XRD) patterns were obtained using the Rigaku SmartLab 9KW X-ray diffractometer. Transmission electron microscopy (TEM) was performed on a JEM1400 microscope. Scanning electron microscopy (SEM) and energy-dispersive Xray (EDX) characterization were conducted with the Zeiss Sigma 300 instrument. High resolution transmission electron microscopy (HRTEM) images were acquired using the JEM-2100 microscope. High-angle annular dark field (HAADF)-

scanning transmission electron microscopy (STEM) and energy-dispersive X-ray (EDX) were tested on the FEI Titan G2 60-300. X-ray photoelectron spectroscopy (XPS) measurements were performed by a Thermo Fisher ESCALAB XI. High performance liquid chromatography (HPLC) analysis was performed using an Agilent G7114A system.

Electrochemical measurements

The electrochemical tests were conducted using a CHI760E workstation. All electrochemical measurements employed the three-electrode system, which comprised a catalyst-loaded carbon paper as the working electrode, platinum foil as the counter electrode and saturated Ag/AgCl as the reference electrode. The electrolyte used was 1.0 M KOH solution (10 mL), either with or without 10 mM HMF.

To obtain the catalyst ink, 4 mg of the as-prepared catalyst was combined with Nafion solution (5 wt%, 20 μ L), ethanol (140 μ L) and deionized water (80 μ L). The mixture was subsequently sonicated for 15 minutes to obtain a homogenous suspension. Subsequently, the resulting suspension was casted on a carbon paper ($1 \times 1 \text{ cm}^2$) to act as the working electrode (loading of 4 mg cm^{-2}).

The linear scanning voltammetry (LSV) was performed at 10 mV s^{-1} . The electrochemical double-layer capacitance (Cdl) was measured utilizing cyclic voltammetry (CV). Electrochemical impedance spectroscopy (EIS) characterization was conducted ranging from 1 Hz to 100 kHz.

All potentials in this experiment were referenced to the reversible hydrogen electrode (RHE) using the following formula:

$$E(\text{RHE}) = E(\text{Ag/AgCl}) + 0.197 + 0.059 \times \text{pH} \quad (1)$$

Products analysis

The concentration of different compounds in the electrolysis were monitored by high-performance liquid chromatography (HPLC). During chronoamperometry at 1.45 V, a volume of 10 μL electrolyte was extracted during chronoamperometry, diluted with water to 500 μL , and then analyzed through HPLC. Methanol (30% volume) with ammonium formate (70% volume) aqueous solution (5 mM) was used as the eluent for separation and quantification.

HMF conversion, FDCA yield, and Faraday efficiency (FE) were determined based on the following equations.

$$\text{HMF conversion (\%)} = [\text{n (HMF consumed)} / \text{n (HMF initial)}] \times 100 \quad (2)$$

$$\text{FDCA yield (\%)} = [\text{n (FDCA formed)} / \text{n (HMF initial)}] \times 100 \quad (3)$$

$$\text{Faradaic efficiency (\%)} = [\text{n (FDCA formed)} / (\text{Q} / (6 \times \text{F}))] \times 100 \quad (4)$$

wherein Q is the total transferred charge, F is Faraday constant (96485 C mol^{-1}) and n is the mole number of reactant.

Density functional theory (DFT) Calculation

All DFT calculations were carried out with the Vienna Ab-initio Simulation Package (VASP).^{2,3} The exchange-correlation effects were treated using the Perdew-Burke-Ernzerhof (PBE) functional within the framework of the generalized gradient approximation (GGA).^{4,5} The core-valence interactions were addressed using the projected augmented wave (PAW) method.⁶ Plane wave expansions were truncated at an energy cutoff of 400 eV. Structural optimization was performed with convergence

criteria set at 1.0×10^{-4} eV for energy and 0.05 eV \AA^{-1} for forces. The Brillouin zone was sampled with the $3 \times 3 \times 1$ K-point grid. Dispersion interactions were accounted for using Grimme's DFT-D3 methodology.⁷

The adsorption energy (E_{ads}) between the HMF and the CoO or Cu-CoO is calculated by the following equation:

$$E_{\text{ads}} = E^*_{\text{HMF}} - E_{\text{HMF}} - E_{\text{sub}} \quad (5)$$

where E_{HMF} and E^*_{HMF} denote the energies before and after the adsorption of HMF on the substrates, respectively. E_{sub} represents the energy of CoO and CoO-Cu surfaces.

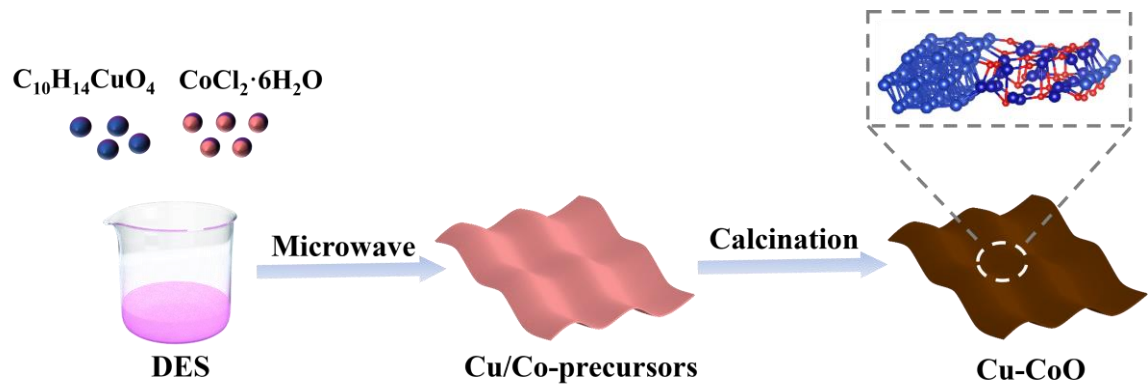


Fig. S1 Schematic diagram of Cu-CoO heterostructure nanosheet synthesis.

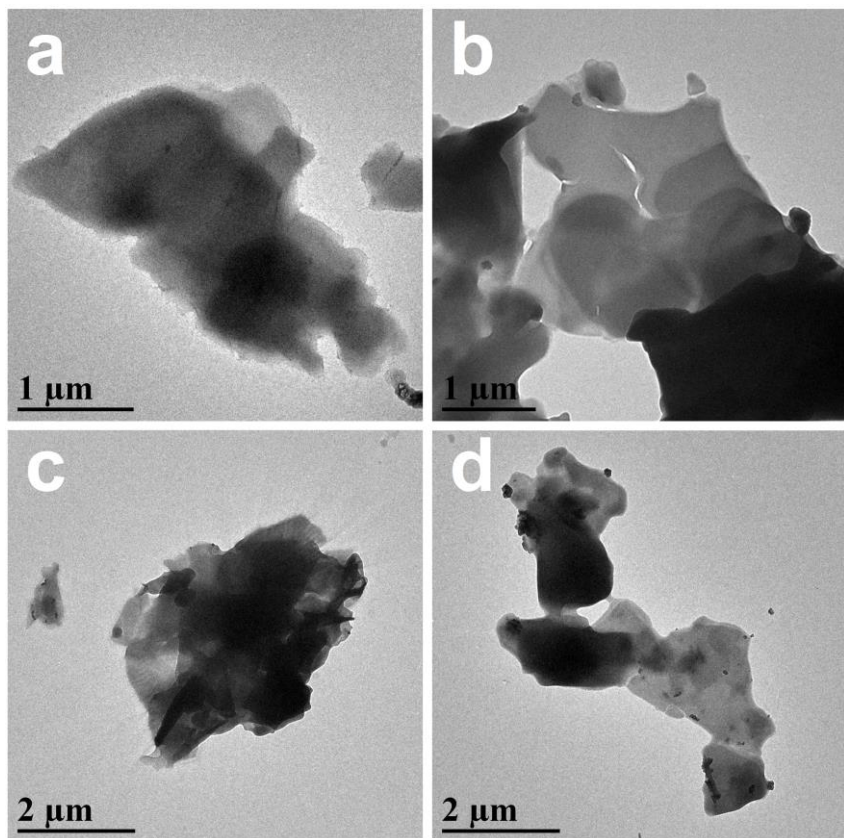


Fig. S2 TEM images of the precursors obtained after microwave heating 1 mL ChCl/OA DES with the presence of $\text{C}_{10}\text{H}_{14}\text{CuO}_4$ and $\text{CoCl}_2 \cdot 6\text{H}_2\text{O}$. (a) Co precursor synthesized with 80 mg $\text{CoCl}_2 \cdot 6\text{H}_2\text{O}$, (b) Cu/Co precursor obtained with the initial mole ratio of Cu/Co=1:2 (51.6 mg $\text{CoCl}_2 \cdot 6\text{H}_2\text{O}$ and 28.4 mg $\text{C}_{10}\text{H}_{14}\text{CuO}_4$), (c) Cu/Co precursor obtained with the initial mole ratio of Cu/Co=1:3 (58.5 mg $\text{CoCl}_2 \cdot 6\text{H}_2\text{O}$ and 21.5 mg $\text{C}_{10}\text{H}_{14}\text{CuO}_4$), (d) Cu/Co precursor obtained with the initial mole ratio of Cu/Co=1:4 (62.7 mg $\text{CoCl}_2 \cdot 6\text{H}_2\text{O}$ and 17.3 mg $\text{C}_{10}\text{H}_{14}\text{CuO}_4$). These obtained precursors will be used for synthesizing CoO, Cu-CoO ($x:y$).

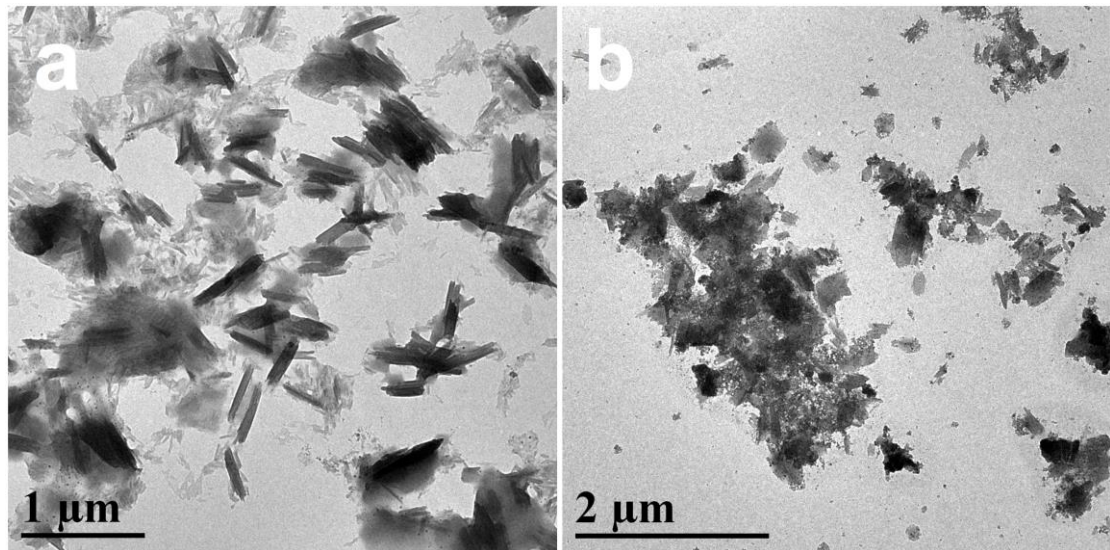


Fig. S3 TEM images of the precursors obtained after (a) 15 s microwave heating, (b) 20 s microwave heating.

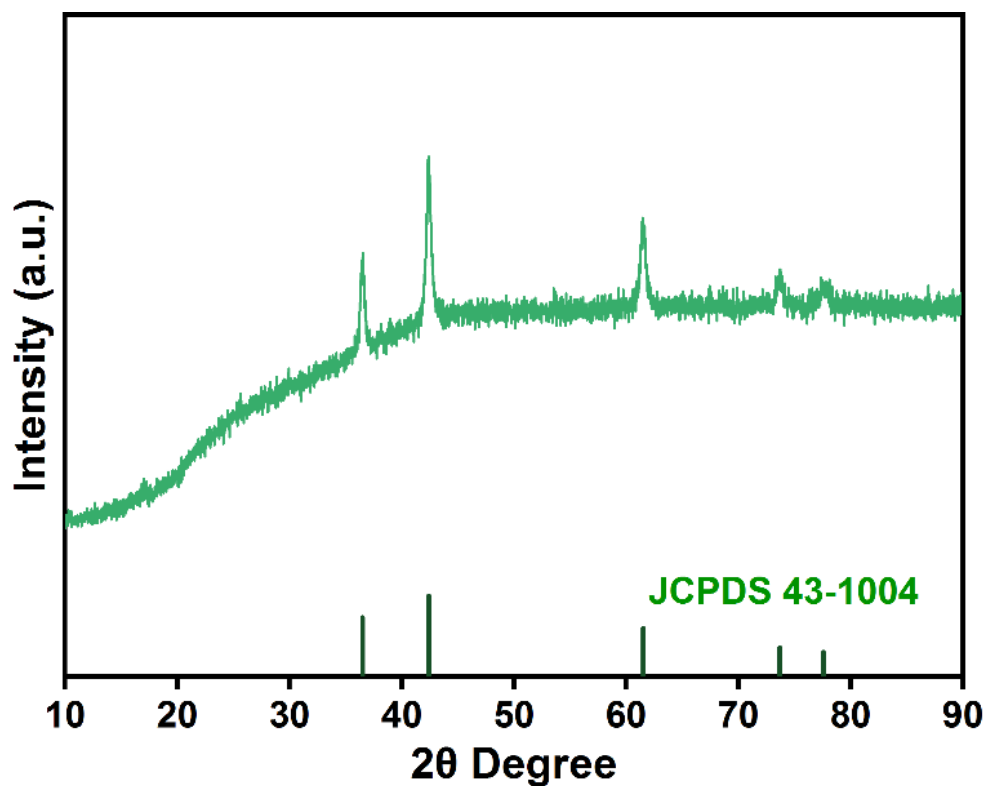


Fig. S4 XRD pattern of the synthesized CoO.

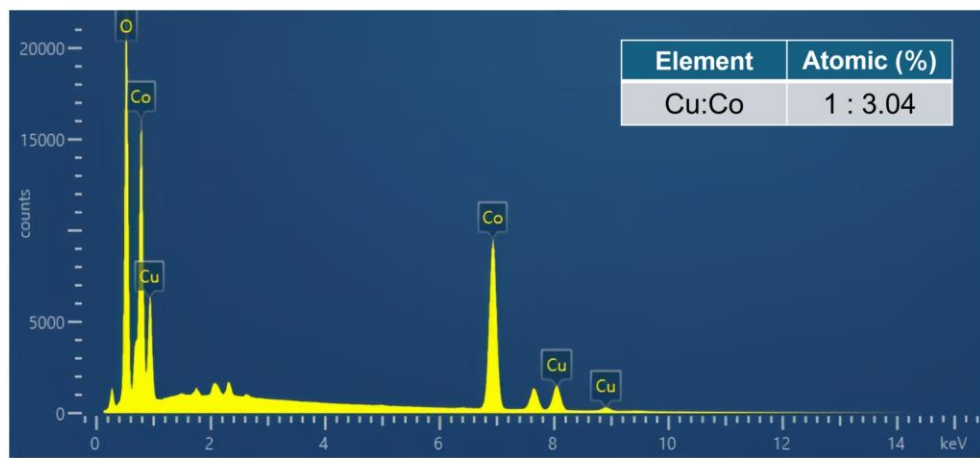


Fig. S5 EDX spectrum of Cu-CoO (1:2) which was synthesized from the precursor obtained after microwave heating 1 mL ChCl/OA DES with 28.4 mg C₁₀H₁₄CuO₄ and 51.6 mg and CoCl₂ 6H₂O.

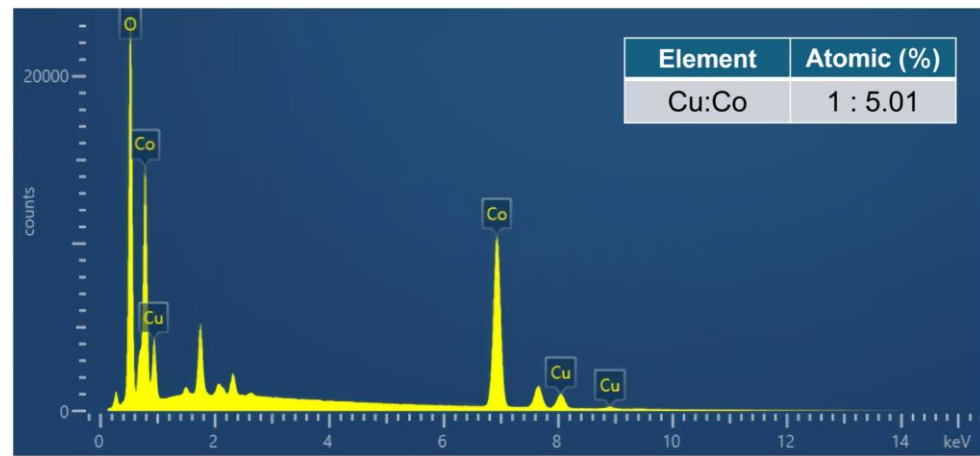


Fig. S6 EDX spectrum of Cu-CoO (1:3) which was synthesized from the precursor obtained after microwave heating 1 mL ChCl/OA DES with 21.5 mg C₁₀H₁₄CuO₄ and 58.5 mg and CoCl₂ 6H₂O.

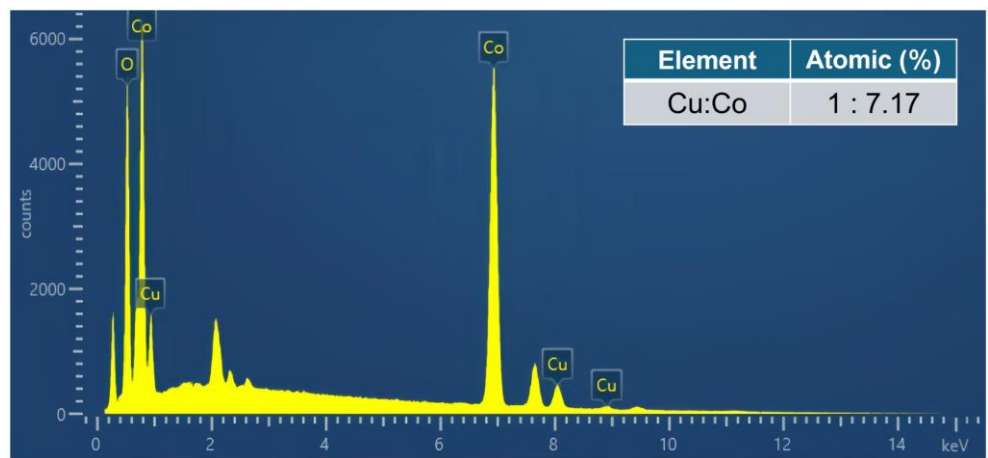


Fig. S7 EDX spectrum of Cu-CoO (1:4) which was synthesized from the precursor obtained after microwave heating 1 mL ChCl/OA DES with 17.3 mg C₁₀H₁₄CuO₄ and 62.7 mg CoCl₂ 6H₂O.

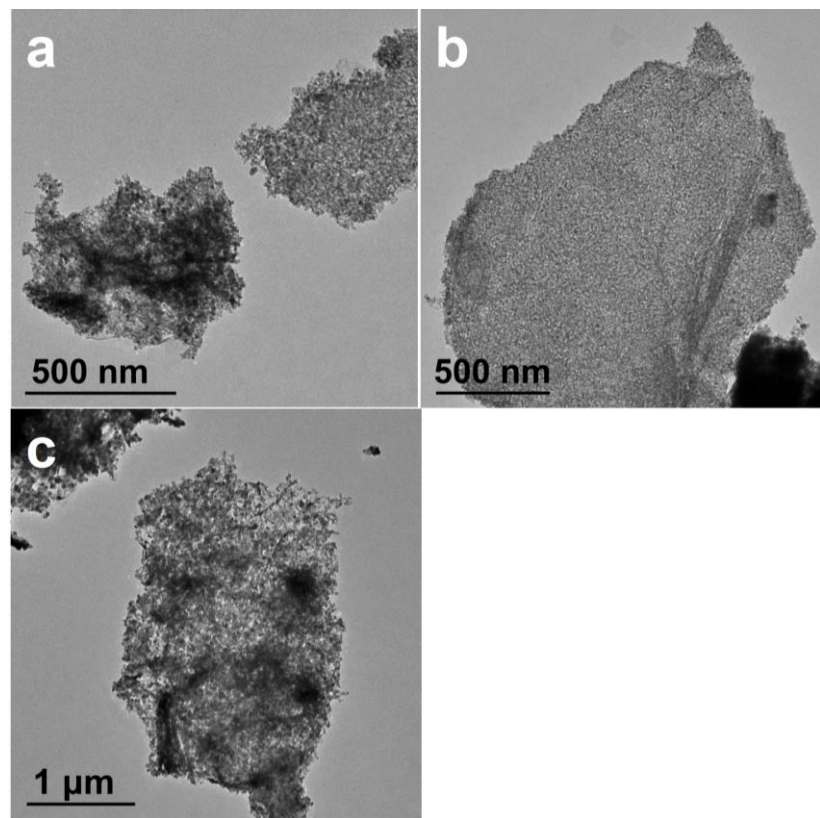


Fig. S8 TEM images of the synthesized (a) CoO, (b) Cu-CoO (1:2), (c) Cu-CoO (1:4).

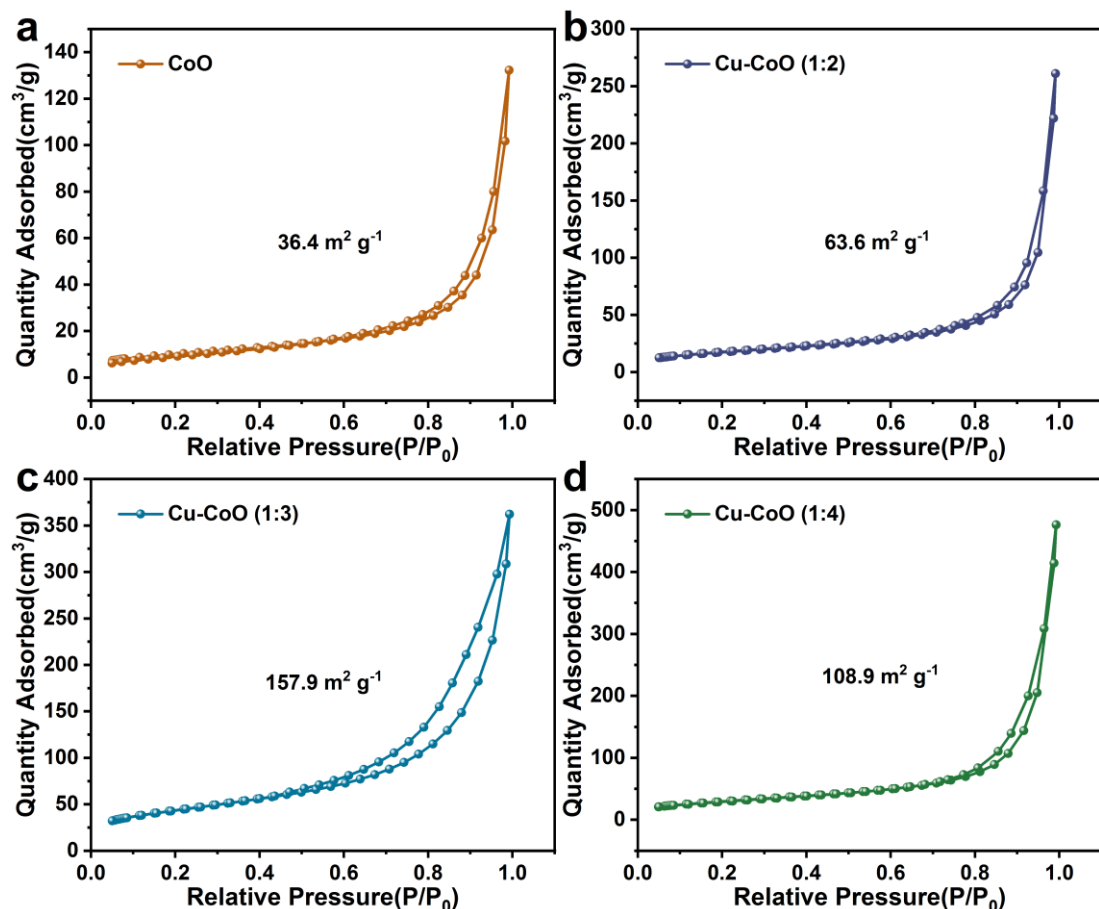


Fig. S9 N₂ adsorption-desorption isotherms of (a) CoO, (b) Cu-CoO (1:2), (c) Cu-CoO (1:3), (d) Cu-CoO (1:4).

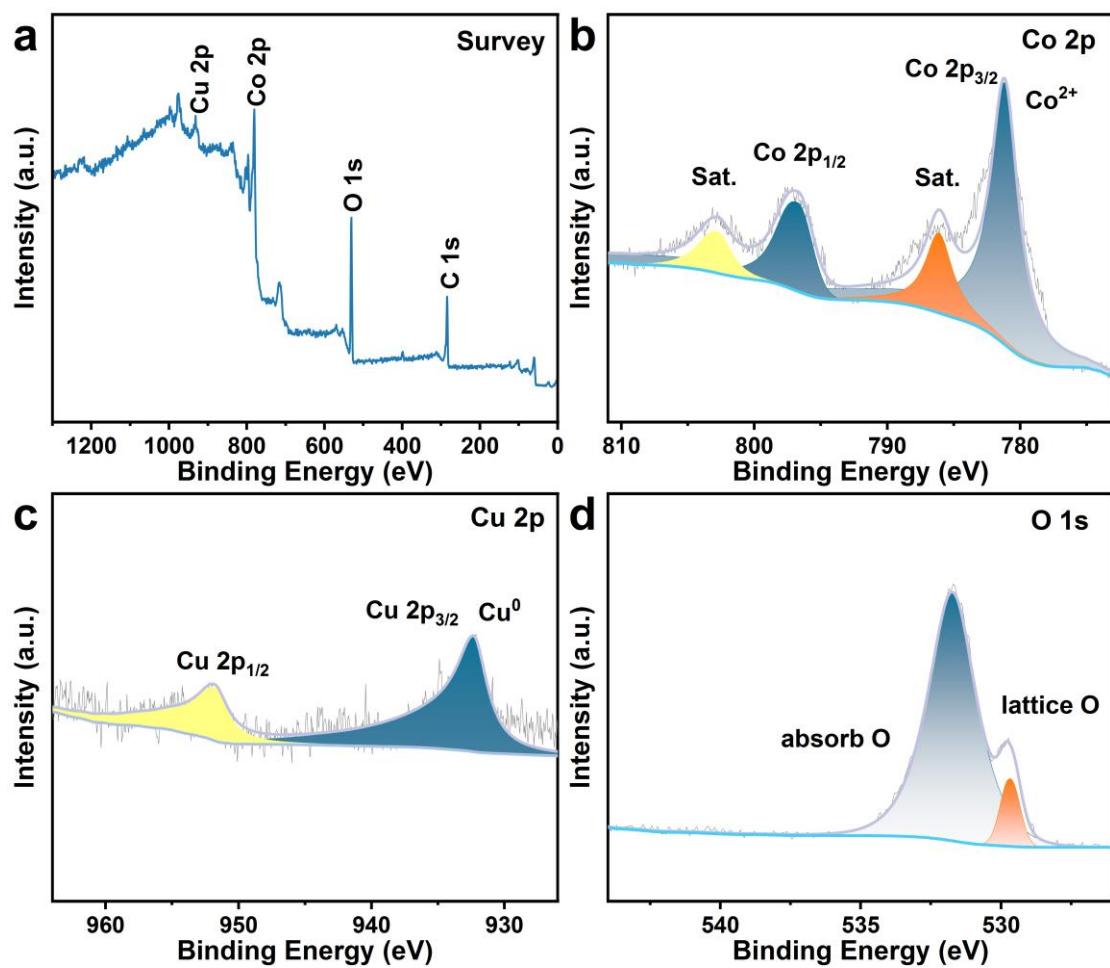


Fig. S10 (a) XPS survey spectrum of Cu-CoO (1:3). High-resolution XPS spectra of (b) Co 2p, (c) Cu 2p, (d) O 1s for the Cu-CoO (1:3).

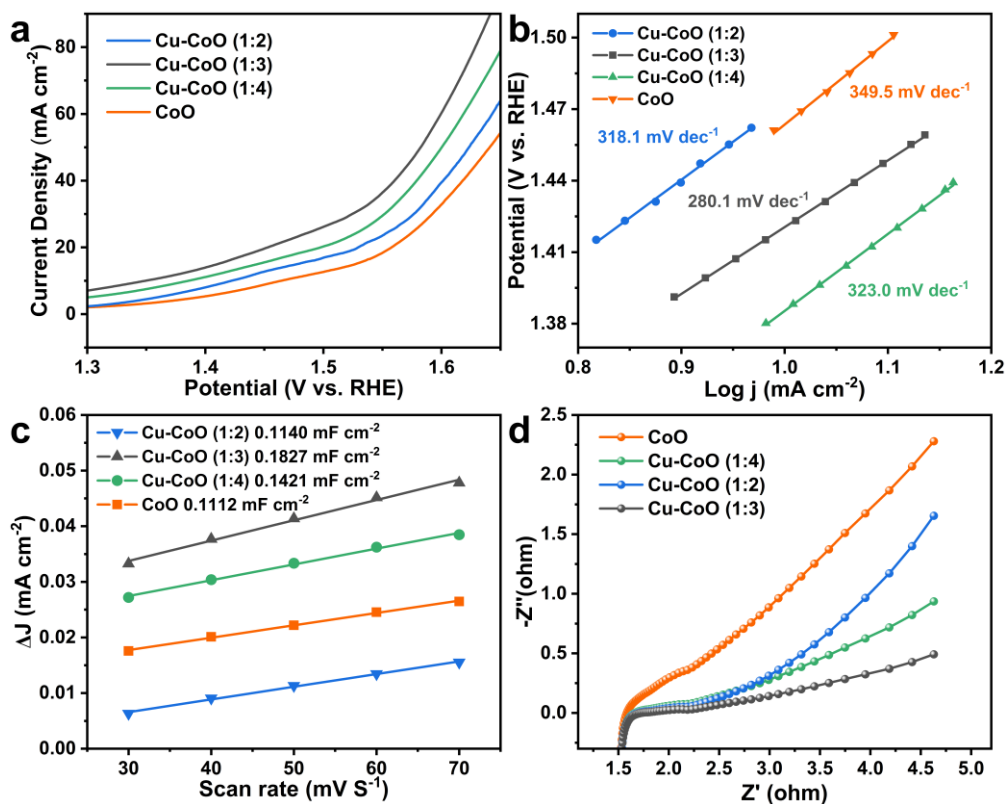


Fig. S11 (a) LSV curves, (b) Tafel plots, (c) electrochemical double layer capacitance (Cdl) of CoO, Cu-CoO (1:2), Cu-CoO (1:3) and Cu-CoO (1:4) in 1.0 M KOH solution with 10 mM HMF and (d) electrochemical impedance spectra of different catalysts at 1.45 V.

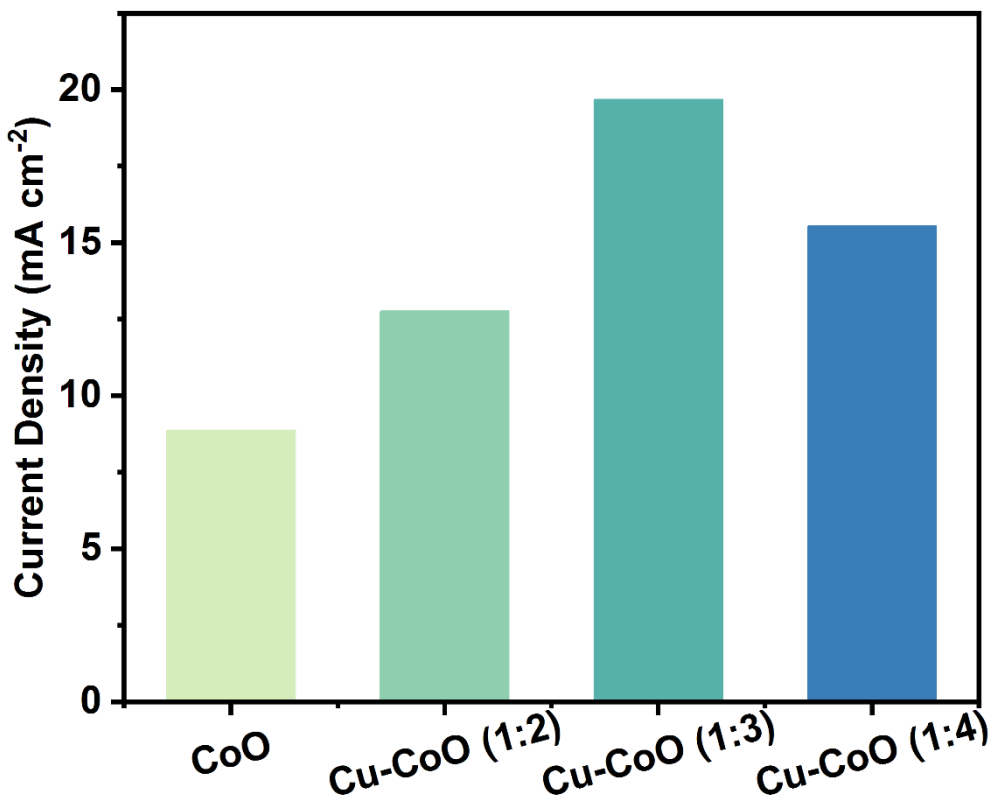


Fig. S12 Corresponding current densities at 1.45 V in 1.0 M KOH with 10 mM HMF.

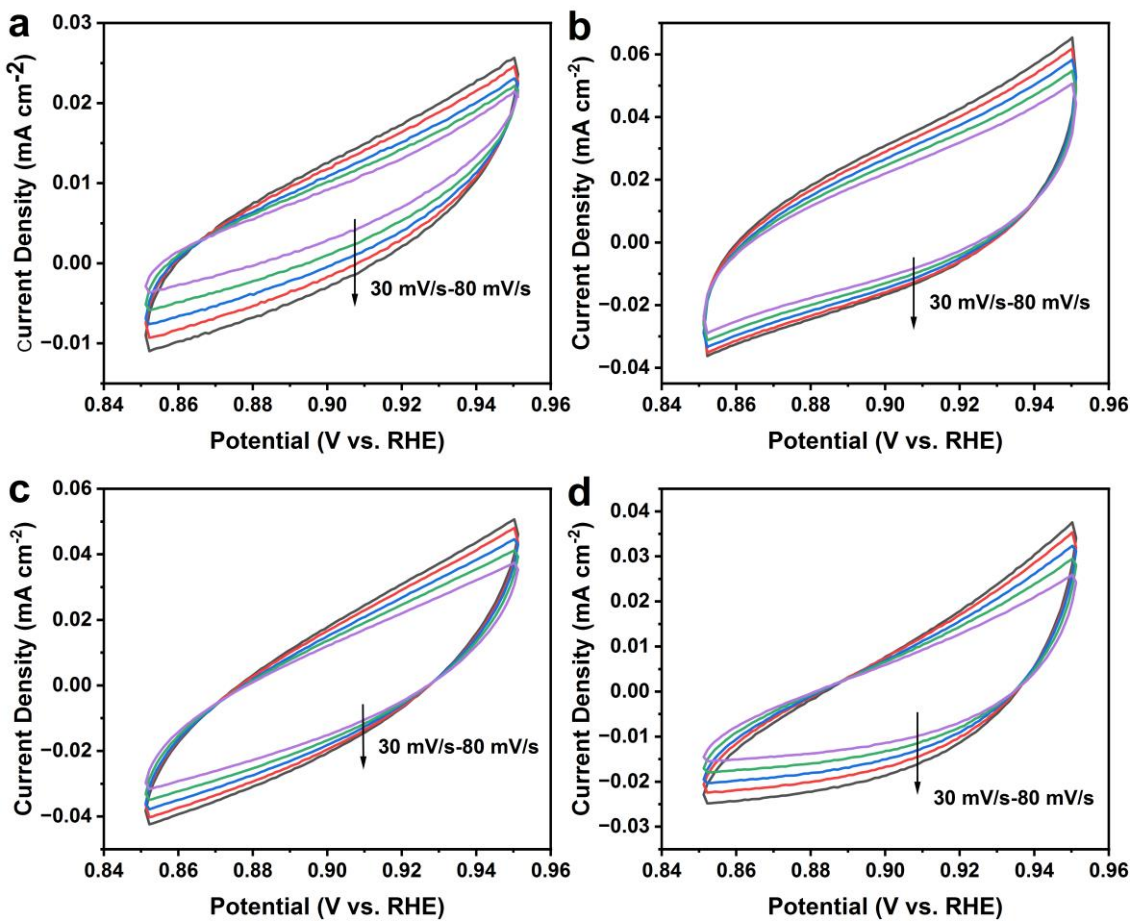


Fig. S13 Cyclic voltammograms of (a) CoO , (b) Cu-CoO (1:2), (c) Cu-CoO (1:3), and (d) Cu-CoO (1:4) at different scan rates from 0.85 to 0.95 V vs. RHE.

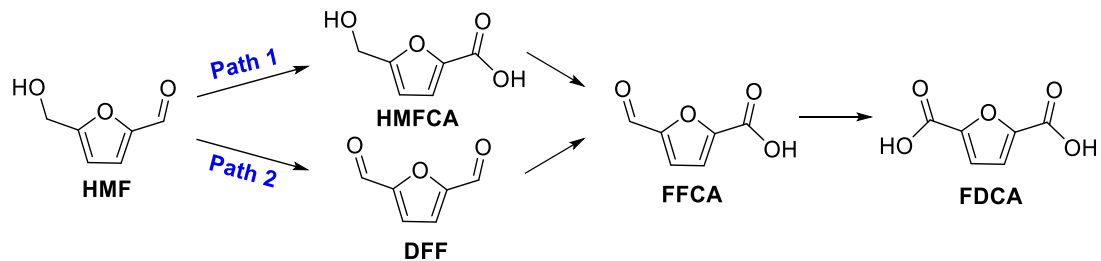


Fig. S14 Possible pathways for the oxidation of HMF to FDCA.

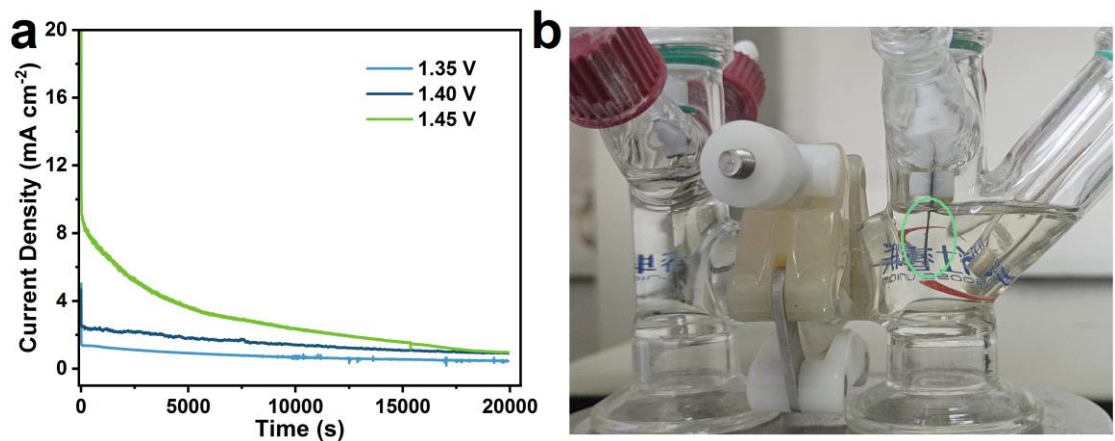


Fig. S15 (a) Corresponding current change over time of the chronoamperometry test of Cu-CoO (1:3) at 1.35 V, 1.40 V and 1.45V, (b) the formed visible oxygen in the electrode at 1.50 V.

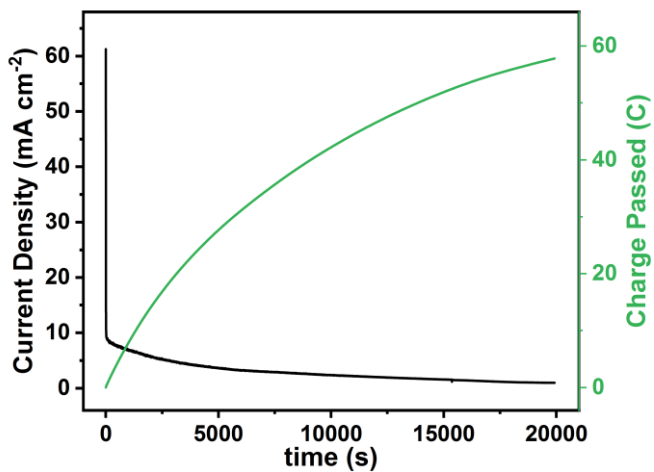


Fig. S16 Corresponding current change and the accumulated charges over time of the chronoamperometry test of Cu-CoO (1:3) at 1.45 V in 1.0 M KOH solution with 10 mM HMF.



Fig. S17 Color change of the recovered electrolyte before and after reaction.

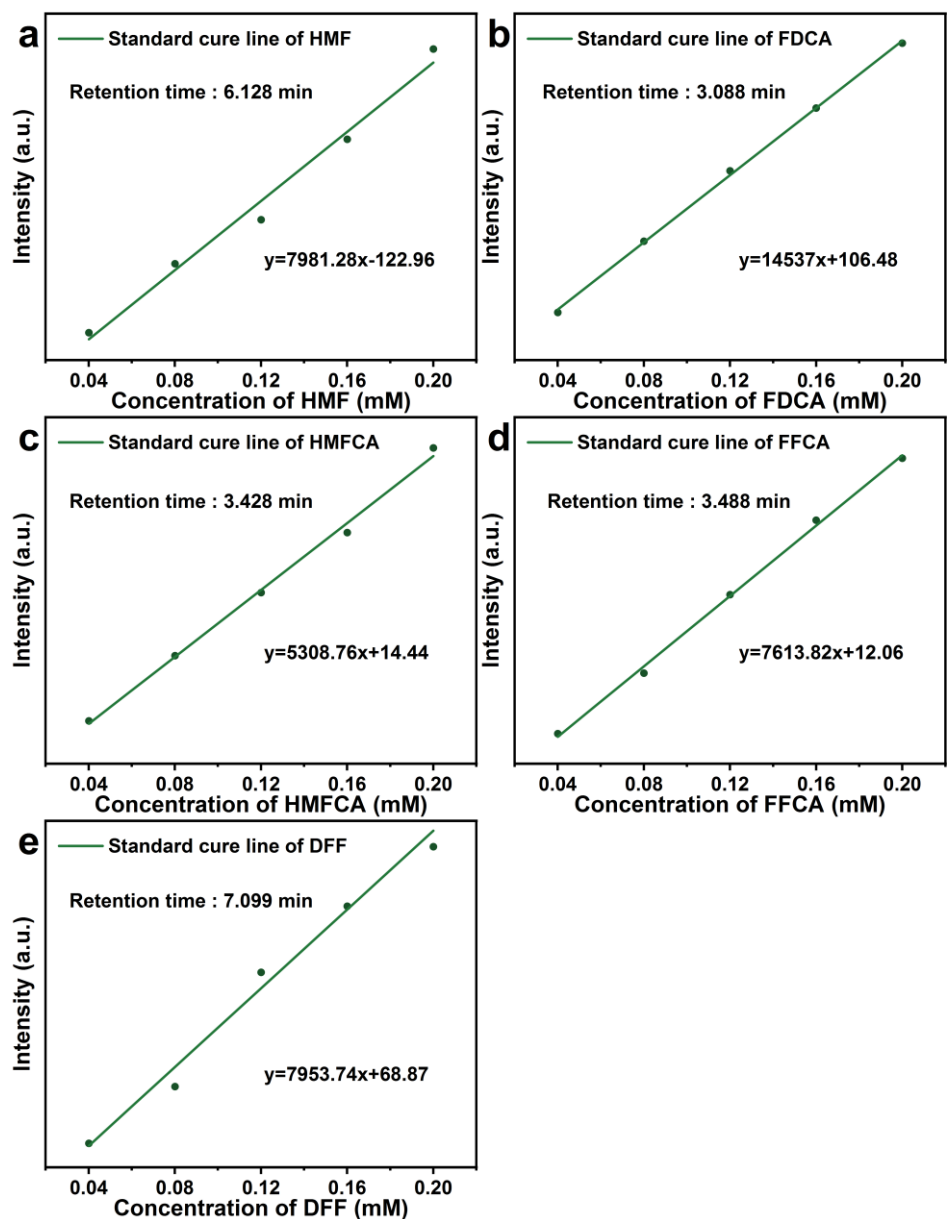


Fig. S18 Standard curves of the HPLC for (a) HMF, (b) FDCA, (c) HMFCA, (d) FFCA and (e) DFF.

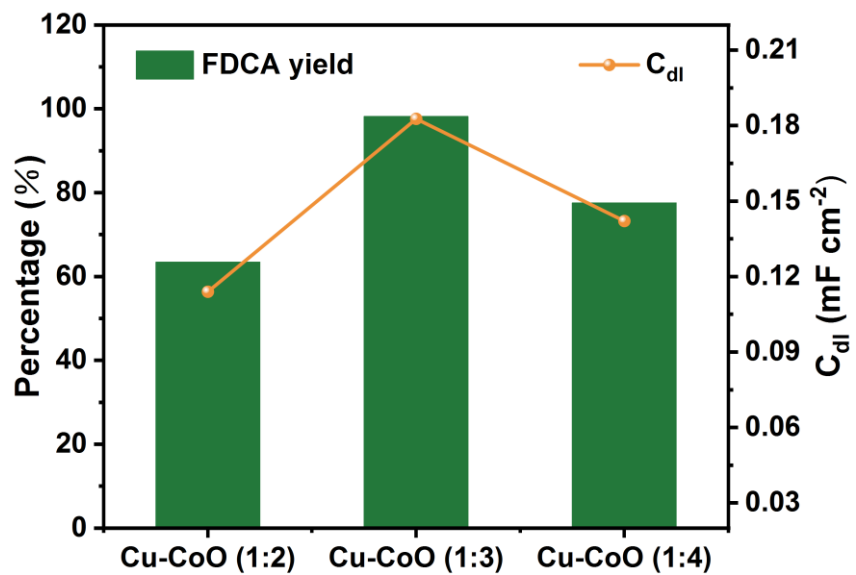
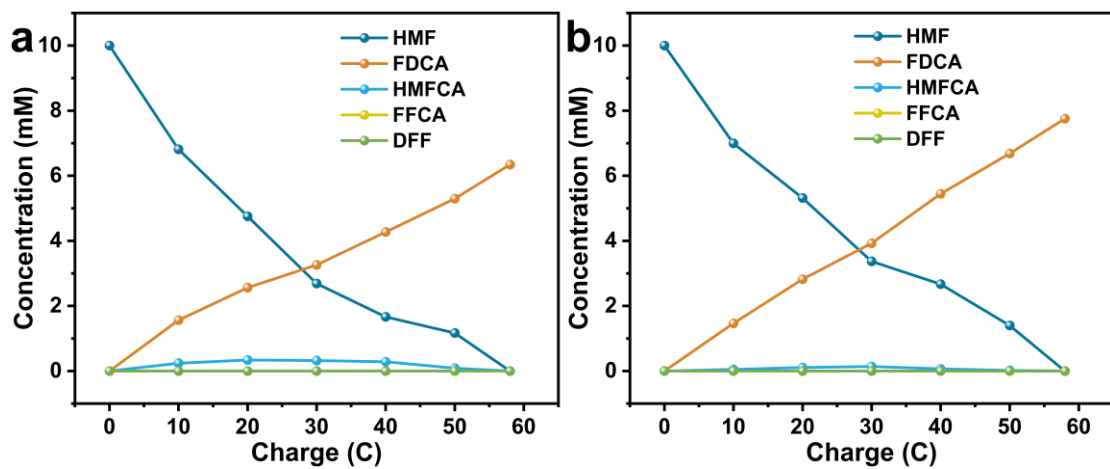


Fig. S20 FDCA yield and C_{dl} of the Cu-CoO (1:2,1:3,1:4).

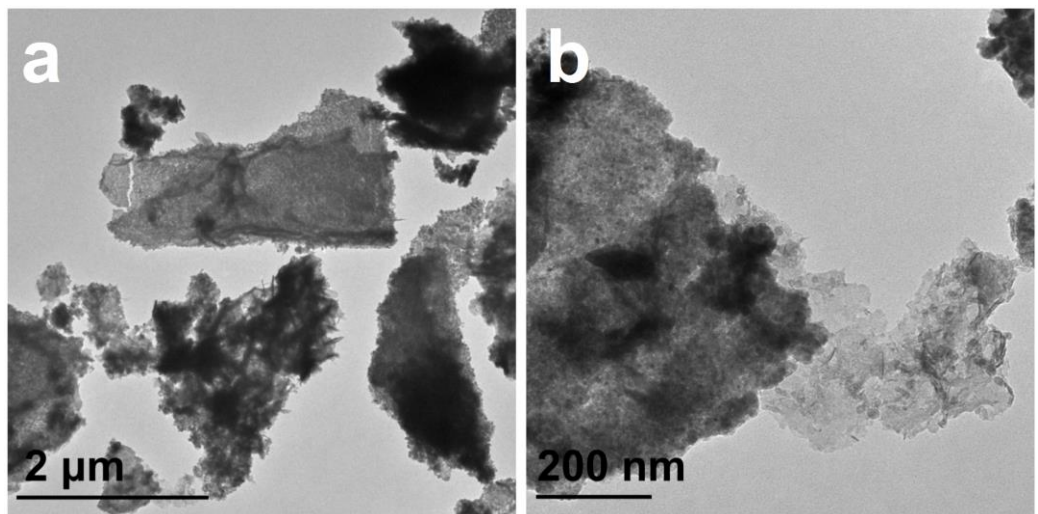


Fig. S21 TEM images of Cu-CoO (1:3) after four electrolysis cycles.

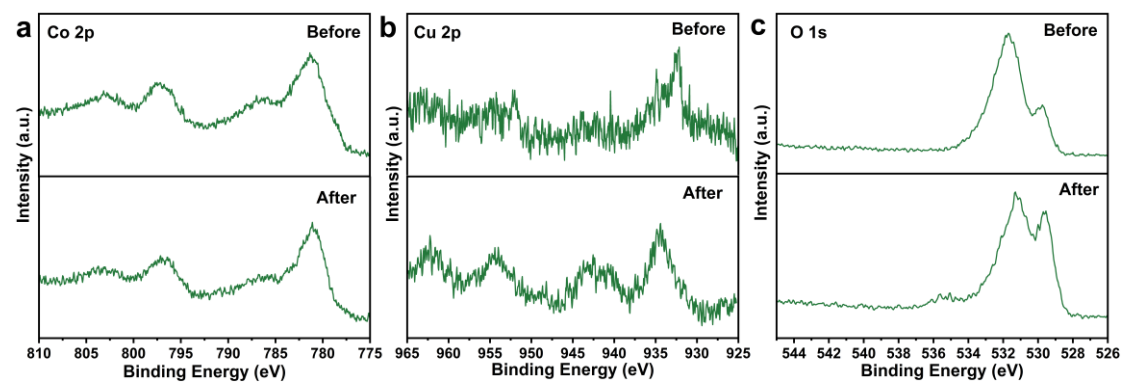


Fig. S22 XPS spectra of (a) Co 2p, (b) Cu 2p, (c) O 1s of Cu-CoO (1:3) before and after four electrolysis cycles.

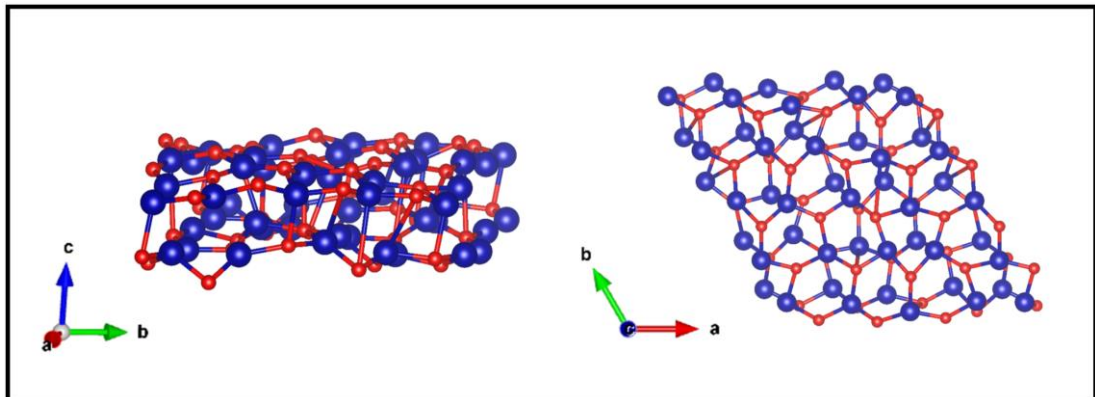


Fig. S23 Side and top views of an optimized structure for the CoO

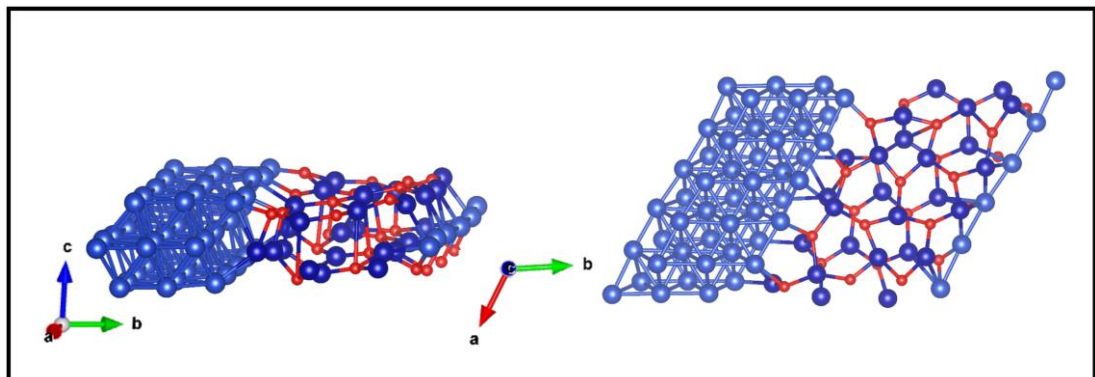


Fig. S24 Side and top views of an optimized structure for the Cu-CoO (1:3).

Table S1 Recently reported electrocatalysts for HMF conversion.

Catalysts	C _{HMF} (mM)	Potential (V vs. RHE)	Conversion (%)	FDCA Yield (%)	FE (%)	Cycles (FDCA yield %)
Cu-CoO (This work)	10	1.45	100	98.2	98.1	4(>95)
nanocrystalline Cu ⁸	5	1.62	99.9	96.4	95.3	5(97.5)
NiCoMn-LDHs ⁹	1	1.50	100	91.7	-	4(>85)
CuH_NWs@Ce:NiH_NSs/Cu ¹⁰	10	1.45	98.5	97.9	98	15(>90)
Cu NPs ¹¹	10	1.47	98	94	-	-
P-Co ₃ O ₄ -NBA@NF ¹²	10	1.636	100	96.9	97.0	30(~90)
Co ₃ O ₄ -NiO-500 ¹³	10	1.45	96.95	83.33	89.47	6(~90)
Co(OH) ₂ @ZIF-67 ¹⁴	10	1.42	90.9	81.8	83.6	3(~80)
CuO-PdO ¹⁵	50	-	99.5	96.2	93.7	6(~90)
CuCo ₂ O ₄ ¹⁶	50	1.45	-	93.7	94	6(~90)
N-NiMoO ₄ ¹⁷	10	1.473	100	97	91	6(~50)
Vo-Sc ₂ O ₃ ¹⁸	10	1.46	-	<95	<90	11(~90)
NiCo ₂ O ₄ ¹⁹	5	1.5	99.6	90.8	87.5	3(>80)
CuNi(OH) ₂ ²⁰	5	1.45	100	93.3	94.4	4(>70)
δ-MnO ₂ ²¹	10	1.457	-	98	98	5(~90)

Table S2 Adsorption energy of HMF on different surfaces

Adsorbed sites	E_{ad/sub}	E_{sub}	E_{ad}
CoO	-526.4025649	-430.52549	-0.73492782
Cu-CoO	-573.2998491	-476.98893	-1.16877207

*Where E_{ad/sub}, E_{ad}, and E_{sub} are the total energies of the optimized adsorbate/substrate system, the adsorbate in the gas phase, and the clean substrate, respectively.

Table S3 Bader charge analysis of Cu-CoO

#	X	Y	Z	CHARGE	MIN DIST	ATOMIC VOL
1	0.4715	1.3230	0.6209	10.7538	0.8282	67.2936
2	1.7507	0.4036	2.6211	10.8649	0.8728	11.8312
3	-0.7075	1.6140	4.7699	11.0028	1.0966	62.0794
4	2.9819	1.1610	0.5460	10.6633	0.8935	66.2919
5	4.2424	0.3299	2.5298	10.8148	0.8633	11.6879
6	1.791	1.6596	4.7064	11.0124	1.087	58.9094
7	5.5142	1.1423	0.4803	10.7147	0.9161	74.2694
8	6.7297	0.0861	2.5488	10.8188	0.8429	11.9081
9	4.2796	1.6473	4.6272	11.0137	1.0751	55.1293
10	8.0186	1.1628	0.5514	10.7572	0.8639	69.1569
11	9.2571	0.0782	2.7288	10.7860	0.8428	12.4325
12	6.7437	1.4855	4.6109	11.0196	1.0863	46.4833
13	10.5112	1.2439	0.6728	10.7788	0.8602	76.0974
14	11.8392	0.2262	2.7435	10.7798	0.9222	12.1675
15	9.2751	1.5264	4.7187	11.0074	1.0883	53.0963
16	-0.7344	3.4464	0.7519	11.0002	1.0966	57.3248
17	0.5235	2.581	2.7759	10.9412	1.0661	11.3428
18	-1.9345	3.8002	4.854	11.0039	1.0816	60.9857
19	1.7960	3.4757	0.7747	11.0164	1.0669	49.7910
20	3.0339	2.5564	2.6878	10.9572	1.0517	11.3316
21	0.5388	3.8321	4.9123	11.0108	1.1027	64.0724
22	4.2877	3.3884	0.6321	10.9976	1.1088	65.8243
23	5.5681	2.4484	2.6249	10.9328	1.0662	11.3027
24	3.0748	3.8395	4.8302	11.0003	1.0858	57.4009
25	6.7841	3.3445	0.6258	10.9958	1.1177	62.6399
26	8.0555	2.3694	2.677	10.9463	1.0826	11.5037
27	5.5600	3.8554	4.7451	11.0081	1.0698	53.5055
28	9.2933	3.3585	0.6771	10.9982	1.0943	59.7942
29	10.5472	2.4464	2.7806	10.9531	1.0750	11.4613
30	8.0466	3.7676	4.7623	11.0118	1.0821	61.4941
31	-1.9331	5.6447	0.9852	10.9979	1.0374	67.7556

32	-0.7077	4.7670	2.8697	10.9826	1.0186	12.0026
33	-3.1242	5.9353	4.7889	10.7259	0.8638	52.9178
34	0.5753	5.6457	0.9851	11.0774	1.0646	57.5410
35	1.8355	4.9414	2.9350	10.8966	1.0301	12.3837
36	-0.5919	6.0944	4.8173	10.7397	0.9043	52.9090
37	3.1026	5.6668	0.9380	11.0743	1.0441	61.0609
38	4.3483	4.6813	2.7529	10.9739	1.0144	11.8841
39	1.8144	5.9452	5.1323	10.9922	1.0519	143.5375
40	5.6267	5.6292	0.9187	11.0447	1.0467	57.7965
41	6.8437	4.6723	2.7649	10.9872	1.0193	11.7728
42	4.1767	6.1177	4.6131	10.7529	0.8786	46.5898
43	8.1046	5.5407	0.8741	11.0624	1.0662	73.7449
44	9.3135	4.6508	2.7992	10.9604	1.0467	12.5438
45	6.8039	6.0395	4.7165	10.7863	0.8870	72.0418
46	-0.3997	7.4949	2.4246	8.3954	0.7663	13.1500
47	-3.8018	9.0780	4.3325	8.1230	0.7461	22.6719
48	1.8524	7.6895	1.7439	8.6589	0.7934	16.1374
49	-1.3704	8.9676	4.2912	8.1542	0.7985	20.2090
50	4.6093	7.7094	2.0982	8.4284	0.8067	13.4046
51	2.1600	8.2207	3.9914	8.1607	0.8010	16.9205
52	7.2301	7.3611	2.4615	8.3753	0.8311	13.7297
53	5.6858	9.1386	3.8694	8.0865	0.7716	16.7844
54	-2.7573	9.7180	2.0133	8.0070	0.7952	17.2648
55	-5.8285	11.8025	3.7828	7.9175	0.7742	12.0202
56	0.2083	10.0646	1.3429	7.9401	0.7578	40.8239
57	-2.4694	11.2420	4.2065	7.9910	0.7637	17.6059
58	3.5052	9.9406	1.0211	7.9714	0.7427	57.5707
59	0.9263	11.3812	4.6004	8.0198	0.7607	41.2115
60	6.6071	9.9115	1.6723	8.0326	0.8169	21.3940
61	3.3374	11.5465	4.2458	8.1188	0.7858	18.8069
62	-4.1201	12.8768	1.5942	7.9528	0.7958	22.5438
63	-7.112	13.8035	4.4002	8.3361	0.7504	21.8184
64	-0.9577	12.7834	1.6327	7.9535	0.7629	20.0641
65	-3.5498	14.1869	4.4218	8.3774	0.7341	22.3349
66	2.3216	12.7933	2.1262	8.1051	0.7484	12.7008

67	-0.9268	14.1108	4.5480	8.4189	0.7375	21.6334
68	4.9854	13.0308	1.7760	8.0502	0.8048	15.0476
69	2.0933	13.7248	4.5509	8.4228	0.7389	19.0992
70	-2.6364	7.7590	4.8311	6.9687	0.7543	87.9806
71	-4.3831	8.8117	1.5814	7.0071	0.7846	42.4197
72	0.2397	7.8817	4.2146	7.0018	0.8664	15.9572
73	-1.1579	8.8653	1.3887	6.9966	0.7793	52.0754
74	4.0383	7.9600	3.9316	7.0048	0.8306	15.2390
75	1.8081	9.2577	0.8181	6.9388	0.7602	120.3803
76	7.0849	7.9661	4.3680	7.0342	0.7730	36.9501
77	5.0773	9.0687	0.8947	6.9390	0.7460	116.7475
78	-4.2744	10.8459	4.3678	6.9580	0.7932	44.6089
79	-5.8321	11.8529	1.7989	7.0887	0.9188	20.7094
80	-0.7086	10.6362	4.3210	6.9272	0.7723	22.5030
81	-2.6282	11.7162	2.0022	7.0848	0.8036	18.6740
82	2.1813	10.0970	4.3625	6.9304	0.7393	41.1178
83	0.5789	11.7728	1.7132	6.9990	0.7590	19.9608
84	5.0753	10.8252	4.2222	6.9909	0.7883	35.9348
85	3.6765	11.6771	1.4478	6.9865	0.7701	23.8242
86	-5.3145	13.6206	4.5682	6.9498	0.7623	58.6868
87	-7.3018	14.5766	0.8163	6.9532	0.8099	67.3168
88	-2.2989	12.9716	4.8975	6.8756	0.7199	94.9684
89	-4.3495	14.4926	0.7191	6.9826	0.8047	90.7623
90	0.4810	13.0878	5.0660	6.9019	0.7311	116.2263
91	-1.3141	14.3373	0.7777	6.9658	0.7719	90.4596
92	3.7950	13.2155	5.0243	6.9379	0.7365	126.8244
93	1.9167	14.4016	1.3432	6.9635	0.7894	24.4527

Table S4 Unit-cell and position parameters of CoO optimization model.

CoO			
Atom Coordinates	x	y	z
Co1	0.97231	0.01794	0.18637
Co2	0.19904	0.08491	0.09766
Co3	0.23987	0.00878	0.19308
Co4	0.41180	0.05548	0.09536
Co5	0.96786	0.22149	0.19680
Co6	0.16465	0.34675	0.07841
Co7	0.26326	0.25648	0.18521
Co8	0.41292	0.29016	0.09975
Co9	0.46921	0.9736	0.21527
Co10	0.71145	0.09508	0.08685
Co11	0.77352	0.02382	0.19741
Co12	0.91013	0.08145	0.09762
Co13	0.51995	0.26866	0.22299
Co14	0.66676	0.31803	0.12813
Co15	0.72011	0.27038	0.22604
Co16	0.94125	0.31726	0.09824
Co17	0.00820	0.51100	0.20457
Co18	0.16785	0.54012	0.10879
Co19	0.21372	0.49774	0.20588
Co20	0.46574	0.59911	0.08902
Co21	0.98213	0.75418	0.20301
Co22	0.21139	0.84417	0.09625
Co23	0.25808	0.77301	0.19836

Co24	0.42069	0.85227	0.11519
Co25	0.49535	0.52529	0.19041
Co26	0.67596	0.60549	0.10816
Co27	0.72171	0.47973	0.21392
Co28	0.92418	0.60429	0.11834
Co29	0.47323	0.77883	0.21020
Co30	0.66213	0.79902	0.07711
Co31	0.71710	0.71785	0.20072
Co32	0.94045	0.81856	0.10300
O1	0.01519	0.00120	0.09926
O2	0.09460	0.18211	0.20500
O3	0.25666	0.99312	0.05909
O4	0.34390	0.17664	0.21892
O5	0.00671	0.23250	0.05667
O6	0.05068	0.38620	0.22359
O7	0.24748	0.25895	0.10024
O8	0.31842	0.42910	0.20179
O9	0.54080	0.01467	0.09532
O10	0.55610	0.14161	0.23582
O11	0.74974	0.97352	0.06732
O12	0.80600	0.18430	0.21565
O13	0.51982	0.23125	0.08665
O14	0.55222	0.43075	0.23025
O15	0.76869	0.26331	0.09193
O16	0.84359	0.43433	0.23409
O17	0.99517	0.49383	0.11824
O18	0.08439	0.68446	0.21983
O19	0.29004	0.51237	0.07868
O20	0.31084	0.66177	0.22644
O21	0.03891	0.74811	0.08234
O22	0.06372	0.93135	0.20757
O23	0.24861	0.71772	0.11941
O24	0.30551	0.92310	0.23390
O25	0.50086	0.46953	0.10014

O26	0.55615	0.68749	0.21849
O27	0.75007	0.49850	0.12367
O28	0.81598	0.65735	0.23018
O29	0.49939	0.76325	0.08820
O30	0.60238	0.94174	0.21077
O31	0.78065	0.75302	0.06917
O32	0.80474	0.89193	0.19923

Table S5 Unit-cell and position parameters of Cu-CoO (1:3) optimization model.

Cu-CoO (1:3)			
Atom Coordinates	x	y	z
Cu1	0.09875	0.08830	0.02920
Cu2	0.15858	0.02694	0.12328
Cu3	0.01793	0.10773	0.22435
Cu4	0.29195	0.07749	0.02568
Cu5	0.35436	0.02202	0.11899
Cu6	0.21976	0.11077	0.22136
Cu7	0.49352	0.07624	0.02259
Cu8	0.54194	0.00574	0.11988
Cu9	0.41813	0.10995	0.21764
Cu10	0.69466	0.07761	0.02593
Cu11	0.74361	0.00522	0.12835
Cu12	0.60765	0.09915	0.21687
Cu13	0.89767	0.08303	0.03164
Cu14	0.95685	0.01510	0.12904
Cu15	0.81189	0.10188	0.22194
Cu16	0.10036	0.23004	0.03536
Cu17	0.16097	0.17227	0.13056
Cu18	0.02075	0.25365	0.22830
Cu19	0.30398	0.23199	0.03644
Cu20	0.36051	0.17063	0.12642
Cu21	0.21993	0.25577	0.23104
Cu22	0.49914	0.22616	0.02973
Cu23	0.55811	0.16342	0.12346
Cu24	0.42300	0.25627	0.22718

Cu25	0.69668	0.22323	0.02943
Cu26	0.75330	0.15815	0.12591
Cu27	0.62240	0.25733	0.22318
Cu28	0.89790	0.22416	0.03185
Cu29	0.95604	0.16328	0.13078
Cu30	0.81713	0.25147	0.22399
Cu31	0.10599	0.37676	0.04634
Cu32	0.16344	0.31818	0.13497
Cu33	0.02418	0.39615	0.22524
Cu34	0.30655	0.37683	0.04633
Cu35	0.37479	0.32982	0.13804
Cu36	0.23396	0.40678	0.22658
Cu37	0.50956	0.37824	0.04412
Cu38	0.56366	0.31246	0.12948
Cu39	0.41943	0.39681	0.24139
Cu40	0.70960	0.37573	0.04321
Cu41	0.76272	0.31185	0.13004
Cu42	0.61624	0.40833	0.21697
Cu43	0.90359	0.36981	0.04111
Cu44	0.95916	0.31042	0.13166
Cu45	0.82264	0.40311	0.22183
Co1	0.31396	0.50025	0.11404
Co2	0.11507	0.60592	0.20377
Co3	0.50297	0.51324	0.08202
Co4	0.30433	0.59855	0.20183
Co5	0.72428	0.51457	0.09869
Co6	0.55208	0.54870	0.18773
Co7	0.91771	0.49132	0.11577
Co8	0.87629	0.60996	0.18199
Co9	0.22810	0.64863	0.09469
Co10	0.07879	0.78777	0.17792
Co11	0.48117	0.67177	0.06316
Co12	0.32145	0.75036	0.19785
Co13	0.73899	0.66349	0.04802
Co14	0.59933	0.75965	0.21637

Co15	0.98561	0.66155	0.07865
Co16	0.79970	0.77068	0.19970
Co17	0.26495	0.85947	0.07498
Co18	0.06854	0.92132	0.20696
Co19	0.51343	0.85324	0.07679
Co20	0.37100	0.94691	0.20797
Co21	0.77604	0.85390	0.10000
Co22	0.57717	0.94183	0.21391
Co23	0.99993	0.86975	0.08353
Co24	0.80078	0.91607	0.21404
O1	0.14735	0.51788	0.22723
O2	0.05631	0.58814	0.07438
O3	0.38292	0.52607	0.19823
O4	0.31660	0.59172	0.06531
O5	0.69019	0.53130	0.18492
O6	0.57181	0.61791	0.03848
O7	0.93402	0.53171	0.20544
O8	0.82442	0.60530	0.04208
O9	0.15888	0.72391	0.20543
O10	0.08083	0.79113	0.08461
O11	0.43425	0.70992	0.20323
O12	0.33064	0.78201	0.09417
O13	0.64037	0.67393	0.20518
O14	0.58962	0.78578	0.08058
O15	0.90533	0.72254	0.19859
O16	0.83283	0.77939	0.06810
O17	0.20379	0.90911	0.21486
O18	0.08905	0.97292	0.03839
O19	0.41490	0.86580	0.23035
O20	0.32118	0.96732	0.03382
O21	0.64249	0.87356	0.23827
O22	0.55666	0.95695	0.03658
O23	0.91331	0.88208	0.23631
O24	0.81790	0.96125	0.06317

Table S6 Unit-cell and position parameters of the optimized model for the adsorption of HMF on CoO

HMF@CoO				
	Atom Coordinates	x	y	z
a (Å)			12.05760	
b (Å)			12.05760	
c (Å)			23.69190	
α (deg)			90.0000	
β (deg)			90.0000	
γ (deg)			120.0000	
Co1		0.97231	0.01794	0.18637
Co2		0.19904	0.08491	0.09766
Co3		0.23987	0.00878	0.19308
Co4		0.41180	0.05547	0.09536
Co5		0.96786	0.22149	0.19680
Co6		0.16465	0.34675	0.07841
Co7		0.26326	0.25647	0.18521
Co8		0.41292	0.29016	0.09975
Co9		0.46921	0.97360	0.21527
Co10		0.71146	0.09508	0.08685
Co11		0.77352	0.02382	0.19741
Co12		0.91013	0.08145	0.09762
Co13		0.51995	0.26866	0.22299
Co14		0.66676	0.31803	0.12813
Co15		0.72011	0.27037	0.22604
Co16		0.94125	0.31726	0.09824
Co17		0.00820	0.51100	0.20457
Co18		0.16785	0.54012	0.10879
Co19		0.21372	0.49774	0.20588
Co20		0.46574	0.59911	0.08902
Co21		0.98213	0.75418	0.20301
Co22		0.21139	0.84417	0.09625

Co23	0.25808	0.77301	0.19836
Co24	0.42069	0.85226	0.11519
Co25	0.49535	0.52529	0.19041
Co26	0.67596	0.60549	0.10816
Co27	0.72171	0.47973	0.21392
Co28	0.92418	0.60429	0.11834
Co29	0.47323	0.77883	0.21020
Co30	0.66213	0.79902	0.07711
Co31	0.71710	0.71785	0.20072
Co32	0.94045	0.81856	0.10300
O1	0.01519	0.00120	0.09926
O2	0.09460	0.18211	0.20500
O3	0.25666	0.99312	0.05909
O4	0.34390	0.17664	0.21892
O5	0.00671	0.23250	0.05667
O6	0.05068	0.38620	0.22359
O7	0.24748	0.25895	0.10023
O8	0.31842	0.42910	0.20180
O9	0.54080	0.01467	0.09532
O10	0.55610	0.14161	0.23582
O11	0.74974	0.97352	0.06732
O12	0.80600	0.18430	0.21565
O13	0.51982	0.23125	0.08665
O14	0.55222	0.43075	0.23025
O15	0.76869	0.26331	0.09193
O16	0.84359	0.43433	0.23409
O17	0.99517	0.49383	0.11824
O18	0.08439	0.68446	0.21983
O19	0.29004	0.51237	0.07868
O20	0.31084	0.66177	0.22644
O21	0.03891	0.74811	0.08234
O22	0.06372	0.93135	0.20757
O23	0.24861	0.71772	0.11941
O24	0.30551	0.92310	0.23390
O25	0.50086	0.46953	0.10014

O26	0.55615	0.68749	0.21849
O27	0.75007	0.49850	0.12367
O28	0.81598	0.65735	0.23018
O29	0.49939	0.76325	0.08820
O30	0.60238	0.94174	0.21077
O31	0.78065	0.75302	0.06917
O32	0.80474	0.89193	0.19923
O33	0.54723	0.61036	0.35021
O34	0.47936	0.80254	0.32919
O35	0.64881	0.37191	0.35880
C1	0.42272	0.58694	0.34966
C2	0.33946	0.45697	0.35641
C3	0.41547	0.39814	0.36127
C4	0.54108	0.49557	0.35761
C5	0.66574	0.49729	0.36052
C6	0.39821	0.69074	0.34073
H1	0.23550	0.41048	0.35662
H2	0.38405	0.29730	0.36665
H3	0.73031	0.56062	0.32692
H4	0.29450	0.66029	0.34375
H5	0.71392	0.53921	0.40093
H6	0.61611	0.33535	0.32138

Table S7 Unit-cell and position parameters of the optimized model for the adsorption of HMF on Cu-CoO (1:3)

HMF@Cu-CoO (1:3)			
Atom Coordinates	x	y	z
Cu1	0.09875	0.08830	0.02920
Cu2	0.15858	0.02694	0.12328
Cu3	0.01793	0.10773	0.22435
Cu4	0.29195	0.07749	0.02568
Cu5	0.35436	0.02202	0.11899
Cu6	0.21977	0.11077	0.22136
Cu7	0.49352	0.07624	0.02259
Cu8	0.54194	0.00574	0.11988
Cu9	0.41813	0.10995	0.21763
Cu10	0.69466	0.07761	0.02593
Cu11	0.74361	0.00522	0.12835
Cu12	0.60765	0.09915	0.21686
Cu13	0.89767	0.08303	0.03164
Cu14	0.95685	0.01509	0.12904
Cu15	0.81189	0.10188	0.22194
Cu16	0.10036	0.23003	0.03536
Cu17	0.16097	0.17227	0.13056
Cu18	0.02075	0.25365	0.22830
Cu19	0.30398	0.23199	0.03644
Cu20	0.36051	0.17063	0.12642
Cu21	0.21993	0.25577	0.23104
Cu22	0.49914	0.22616	0.02973

Cu23	0.55811	0.16342	0.12346
Cu24	0.42300	0.25627	0.22718
Cu25	0.69667	0.22323	0.02943
Cu26	0.75330	0.15815	0.12591
Cu27	0.62240	0.25733	0.22318
Cu28	0.89790	0.22416	0.03185
Cu29	0.95604	0.16328	0.13078
Cu30	0.81713	0.25147	0.22399
Cu31	0.10599	0.37676	0.04634
Cu32	0.16344	0.31818	0.13497
Cu33	0.02418	0.39615	0.22524
Cu34	0.30655	0.37683	0.04633
Cu35	0.37479	0.32982	0.13804
Cu36	0.23396	0.40678	0.22657
Cu37	0.50956	0.37824	0.04412
Cu38	0.56366	0.31246	0.12948
Cu39	0.41942	0.39681	0.24139
Cu40	0.70960	0.37573	0.04321
Cu41	0.76272	0.31185	0.13004
Cu42	0.61624	0.40833	0.21697
Cu43	0.90359	0.36981	0.04111
Cu44	0.95916	0.31042	0.13166
Cu45	0.82264	0.40311	0.22183
Co1	0.31396	0.50025	0.11404
Co2	0.11507	0.60592	0.20377
Co3	0.50297	0.51324	0.08202
Co4	0.30433	0.59855	0.20183
Co5	0.72428	0.51457	0.09869
Co6	0.55208	0.54870	0.18773
Co7	0.91771	0.49132	0.11577
Co8	0.87629	0.60996	0.18199
Co9	0.22810	0.64863	0.09469
Co10	0.07879	0.78776	0.17792
Co11	0.48117	0.67177	0.06316
Co12	0.32145	0.75036	0.19785

Co13	0.73899	0.66349	0.04802
Co14	0.59933	0.75965	0.21637
Co15	0.98561	0.66155	0.07865
Co16	0.79970	0.77068	0.19969
Co17	0.26495	0.85947	0.07498
Co18	0.06854	0.92132	0.20695
Co19	0.51343	0.85323	0.07679
Co20	0.37100	0.94691	0.20797
Co21	0.77604	0.85390	0.10000
Co22	0.57717	0.94184	0.21391
Co23	0.99994	0.86975	0.08353
Co24	0.80078	0.91607	0.21404
O1	0.14735	0.51788	0.22723
O2	0.05631	0.58814	0.07438
O3	0.38292	0.52607	0.19823
O4	0.31660	0.59172	0.06531
O5	0.69019	0.53130	0.18492
O6	0.57181	0.61791	0.03848
O7	0.93402	0.53170	0.20544
O8	0.82442	0.60530	0.04208
O9	0.15888	0.72391	0.20543
O10	0.08083	0.79113	0.08461
O11	0.43425	0.70992	0.20323
O12	0.33064	0.78200	0.09417
O13	0.64037	0.67393	0.20518
O14	0.58962	0.78578	0.08058
O15	0.90533	0.72254	0.19859
O16	0.83283	0.77939	0.06810
O17	0.20379	0.90911	0.21486
O18	0.08905	0.97292	0.03839
O19	0.41490	0.86580	0.23035
O20	0.32118	0.96732	0.03382
O21	0.64250	0.87355	0.23827
O22	0.55666	0.95695	0.03658
O23	0.91331	0.88208	0.23631

O24	0.81790	0.96125	0.06317
O25	0.46338	0.54593	0.35120
O26	0.33677	0.64538	0.35587
O27	0.63407	0.42554	0.36380
C1	0.33633	0.50743	0.35313
C2	0.28244	0.41551	0.35263
C3	0.38142	0.39612	0.35108
C4	0.48979	0.47831	0.35058
C5	0.62243	0.50243	0.35595
C6	0.28014	0.56339	0.35576
H1	0.18438	0.36756	0.35634
H2	0.37542	0.33181	0.35763
H3	0.67490	0.54348	0.31503
H4	0.17719	0.52344	0.35749
H5	0.66203	0.54391	0.39827
H6	0.61731	0.39344	0.32325

References

- 1 A. P. Abbott, D. Boothby, G. Capper, D. L. Davies and R. K. Rasheed, *J. Am. Chem. Soc.*, 2004, **126**, 9142-9147.
- 2 G. Kresse and J. Hafner, *Phys. Rev. B*, 1992, **47**, 558-561.
- 3 G. Kresse and J. Hafner, *Phys. Rev. B*, 1994, **49**, 14251-14269.
- 4 J. P. Perdew, K. Burke and M. Ernzerhof, *Phys. Rev. Lett.*, 1996, **77**, 3865-3868.
- 5 G. Kresse and D. Joubert, *Phys. Rev. B*, 1999, **59**, 1758-1775.
- 6 P. E. Blöchl, *Phys. Rev. B*, 1994, **50**, 17953-17979.
- 7 S. Grimme, J. Antony, S. Ehrlich and H. Krieg, *J. Chem. Phys.*, 2010, **132**, 154104.
- 8 D.-H. Nam, B. J. Taitt and K.-S. Choi, *ACS Catal.*, 2018, **8**, 1197-1206.
- 9 B. Liu, S. Xu, M. Zhang, X. Li, D. Decarolis, Y. Liu, Y. Wang, E. K. Gibson, C. R. A. Catlow and K. Yan, *Green Chem.*, 2021, **23**, 4034-4043.
- 10 G. Ren, B. Liu, L. Liu, M. Hu, J. Zhu, X. Xu, P. Jing, J. Wu and J. Zhang, *Inorg. Chem.*, 2023, **62**, 12534-12547.
- 11 Y. Zhou, *Appl. Catal. B-Environ.*, 2022, **317**, 121776.
- 12 D. Liu, Y. Li, C. Wang, H. Yang, R. Wang, S. Li and X. Yang, *Appl. Catal. A-Gen.*, 2024, **669**, 119497.
- 13 P. Jin, L. Zhang, Z. Wu, B. Zhou and Z. Duan, *Chem. Eng. J.*, 2024, **481**, 148303.
- 14 T. Pila, K. Nueangnoraj, S. Ketrat, V. Somjit and K. Kongpatpanich, *ACS Appl. Energy Mater.*, 2021, **4**, 12909-12916.
- 15 P. Zhou, X. Lv, S. Tao, J. Wu, H. Wang, X. Wei, T. Wang, B. Zhou, Y. Lu, T. Frauenheim, X. Fu, S. Wang and Y. Zou, *Adv. Mater.*, 2022, **34**, 2204089.

- 16 Y. Lu, C. Dong, Y. Huang, Y. Zou, Z. Liu, Y. Liu, Y. Li, N. He, J. Shi and S. Wang, *Angew. Chem. Int. Ed.*, 2020, **59**, 19215-19221.
- 17 W. Wang and M. Wang, *Catal. Sci. Technol.*, 2021, **11**, 7326-7330.
- 18 Y. Wu, L. Ma, J. Wu, M. Song, C. Wang and J. Lu, *Adv. Mater.*, 2024, 2311698.
- 19 M. J. Kang, H. Park, J. Jegal, S. Y. Hwang, Y. S. Kang and H. G. Cha, *Appl. Catal. B*, 2019, **242**, 85-91.
- 20 H. Chen, J. Wang, Y. Yao, Z. Zhang, Z. Yang, J. Li, K. Chen, X. Lu, P. Ouyang and J. Fu, *Chemelectrochem*, 2019, **6**, 5797-5801.
- 21 C. Wang, H.-J. Bongard, C. Weidenthaler, Y. Wu and F. Schüth, *Chem. Mater.*, 2022, **34**, 3123-3132.